Decoupled Phase Transitions and Grain-Boundary Melting in Supported Phospholipid Bilayers

Danielle Keller
MEMPHYS, Physics Department, University of Southern Denmark, DK-5230 Odense M, Denmark and Danish Polymer Centre, Risø National Laboratory, DK-4000 Roskilde, Denmark

Niels B. Larsen
Danish Polymer Centre and Plant Research Department, Risø National Laboratory, DK-4000 Roskilde, Denmark

Ian M. Møller
Plant Research Department, Risø National Laboratory, DK-4000 Roskilde, Denmark

Ole G. Mouritsen
MEMPHYS, Physics Department, University of Southern Denmark, DK-5230 Odense M, Denmark
(Received 17 August 2004; published 20 January 2005)

Two separate liquid-solid phase transitions are detected in the two monolayers of a mica-supported phospholipid bilayer by atomic force microscopy. The phase transitions of the two monolayers are decoupled by the stronger interaction between the lipid headgroups of the proximal monolayer and the mica support. The transition temperature of the proximal monolayer is increased and this transition occurs over a narrower temperature range. Both transitions occur via grain-boundary melting and the variation of the width of the interfacial zone with temperature is consistent with mean-field theory.

DOI: 10.1103/PhysRevLett.94.025701 PACS numbers: 64.70.Dv, 68.37.Ps, 68.47.Pe, 87.14.Cc

Supported phospholipid bilayers are widely used as a model system of biological membranes [1,2]. An advantage of the supported layers over vesicles in suspension is that the samples can be investigated by surface-sensitive techniques such as atomic force microscopy (AFM). Vesicles in solution undergo an abrupt first-order phase transition from a low-temperature solid phase to a high-temperature liquid phase at the chain-melting temperature, T_m. When lipids with different phase transition temperatures are mixed, the phase diagram of the mixture contains a region where the solid and liquid phases coexist. It is generally assumed that the thermodynamic properties of vesicles in solution are maintained in supported bilayers, but the effect of the supporting material on the phase transition remains little investigated [3–7]. In one study it was shown by differential scanning calorimetry (DSC) that supported bilayers of 1,2-dipalmitoyl-*sn*-phosphatidylcholine (DPPC) and the C15-carbon chain analogue, respectively, each have two phase transitions which are both slightly higher than for the corresponding one-component vesicles in solution [3]. Other investigations performed with AFM on mica-supported bilayers of 1,2-dimyristoyl-*sn*-phosphatidylcholine (DMPC) [5] and DPPC [6] showed that the phase transitions occur continuously over broad (10 K) temperature ranges where solid and liquid domains coexist.

We have performed a systematic investigation of the properties of supported phospholipid bilayers by AFM. By thermal cycling we were able to monitor the complete solid-to-liquid transition followed by the liquid-to-solid transition in a single AFM experiment by slowly heating and cooling the sample during scanning. Our data show that the phase transition in the top (distal) monolayer is decoupled from the phase transition in the bottom (proximal) monolayer. This decoupling is suggested to be caused by the enhanced interaction between the lipid headgroups of the proximal monolayer and the mica support. We find the solid-to-liquid transition to proceed by grain-boundary melting in a manner consistent with mean-field theory predictions. Our model membranes consist of a binary mixture of the phospholipids DPPC and 1-stearoyl-2-oleoyl-*sn*-phosphatidylcholine (SOPC). We have observed that vesicles of mixtures of DPPC and 10–25% SOPC almost always (in >80% of the preparations) form granular bilayers on mica when the procedure described in the present Letter is applied. Furthermore our results show that both monolayers contain identical grain-boundary patterns consistent with decoupled phase transitions but coupled domain structures. Since only the solid phase monolayers are granular, the presence of grains and grain boundaries can be used as a probe for the solid phase in the proximal monolayer when the distal monolayer has undergone the solid-to liquid transition. We have also observed decoupled phase transitions (as well as grain-boundary melting) in pure DMPC bilayers that happened to be granular after preparation (not shown). However, it is very often found that bilayers of only one lipid component are homogeneous and not granular, and can be prepared without or with only a few holes. In such bilayers decoupled phase transitions may escape notice due to the absence of a granular structure.

We used a mixture of 80 mol % DPPC and 20 mol % SOPC, which has a phase coexistence region in the temperature range from ~27 to ~38 °C in a vesicular phase in

pure water as determined by DSC (6100 N-DSC II, Calorimetry Sciences Corp., Lindon, UT) at a heating rate of 0.5 K/min (not shown). When the phase transitions in the monolayers are decoupled, as is observed in the present study, there will be a phase coexistence region for each monolayer. The phenomenological phase diagram for a supported bilayer therefore contains two coexistence regions as illustrated schematically in Fig. 1.

Experimental procedures.—The lipids dissolved in chloroform were mixed in appropriate amounts. Chloroform was evaporated and the dry lipid film was then suspended in ultrapure water (UPW, Millipore, resistivity 18.2 MΩ cm^{-1}) to a lipid concentration of 1 mg/ml and hydrated at 50 °C for 1 h. Small unilamellar vesicles (SUVs) were prepared by extrusion through two 100 nm polycarbonate filters in a Lipex Extruder (Northern Lipids Inc., Vancouver, Canada). Supported bilayers were prepared by applying the vesicle solution onto a sheet of freshly cleaved mica (Ruby muscovite mica, Plano GmbH, Wetzlar, Germany) and by incubating the sample overnight at 4 °C. After washing off excess unbound vesicles the sample was incubated at 50 °C for 30 min, and subsequently cooled to room temperature (21 °C) and mounted in a homemade AFM fluid cell equipped with a thermocouple to directly measure the temperature inside the cell. AFM images of the samples in UPW water were acquired in MAC mode using a PicoSPM atomic force microscope (Molecular Imaging, Tempe, AZ). The cantilever oscillation frequency in water was ~23 kHz and the nominal spring constant was 2.8 N/m. During the experiments the temperature was adjusted with a Lakeshore model 330 temperature controller (Lake Shore Cryotronics Inc., Westerville, OH). In the heating series the temperature was changed in steps of 2 to 3 K on the temperature controller. The sample was subjected to approximately 30 min of temperature equilibration at each temperature step. Consecutive AFM images on the image scale did not show changes in the domain structure after this time indicative of thermal equilibrium, although we cannot exclude structural processes occurring over hours or longer. Cooling was done in steps of 5 K. In a complete heating-cooling series the sample was scanned continuously for approximately 8 h. Care was taken that the sample remained hydrated during the experiment. Because of thermal drift in the scanner the scanned region is not exactly the same in subsequent images of the temperature cycle but identical surface features can be identified in all adjacent images.

Initially the bilayer typically has holes and line defects [Fig. 1(a)]. The depth of the holes is 5.0 nm corresponding to the thickness of the bilayer in the solid phase and a very thin water film between the bilayer and the mica support [5]. Phase imaging shows a large phase difference between the top of the bilayer and the bottom of the holes (not shown), which indicates that there is only one bilayer supported directly on the mica surface. The line defects are grain boundaries formed during the preparation when

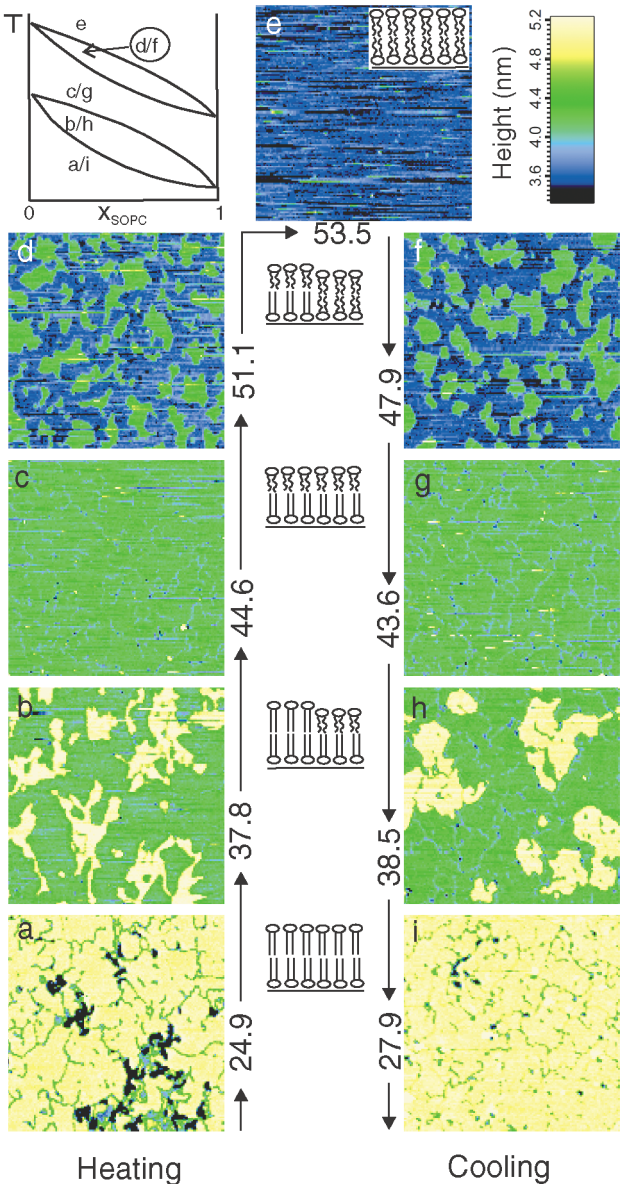

FIG. 1 (color). The phase diagram in the upper left corner has two phase coexistence regions corresponding to one in each monolayer. This is consistent with our AFM data. The transition temperature in pure water of DPPC is 41.3 °C and that of SOPC is 5 °C. Images of a DPPC-SOPC (80/20 mol %) bilayer on a solid mica support at various temperatures in the heating-cooling cycle: (a) at room temperature, the darkest areas are holes and the grain boundaries are clearly visible; (b) during the phase transition of the distal monolayer; (c) when the distal monolayer is completely melted; (d) during the phase transition of the proximal monolayer, and (e) when the bilayer is completely fluid. Images (f)–(i) are corresponding images obtained when the bilayer is cooled. Note the similarity between the defect structure of images (c) and (g) and of (a) and (i). All images are 2.4×2.4 μm^2.

the liquid phase is quenched from a temperature above the phase transition temperature to room temperature, which is much lower than T_m for the mixture with this lipid composition. The solid phase crystallites are irregular in shape

but the angles between boundaries are predominantly around 120 deg. Holes are not always present in the supported bilayers, but the grain-boundary structure is similar in different preparations. The holes reaching down to the mica surface shrink due to lateral bilayer expansion at slightly elevated temperatures.

The solid-to-liquid transition in the distal monolayer is initiated at the grain boundaries. The measured height difference between solid and liquid domains in the distal monolayer is between 6.6 and 7.7 Å, which is slightly more than the expected height difference between a solid and a liquid DPPC monolayer. The difference between solid and liquid DPPC bilayers as determined by x-ray diffraction is 11.2 Å [8]. The liquid areas grow with increasing temperature from the grain boundaries [Fig. 1(b)] until the distal monolayer is completely liquid [Fig. 1(c)]. At this stage the bilayer still has a lateral structure of line defects resembling the structure observed before heating. This is not expected if the whole bilayer is liquid and is evidence that only the distal monolayer has gone through a phase transition. We can visually identify a grain-boundary structure in the solid phase proximal monolayer which is identical to the solid domains in the partly melted distal monolayer (not shown), indicating that the grain-boundary structure is identical in the two monolayers. We observe that the proximal monolayer does not begin to melt until the distal monolayer is completely liquid. This has been observed in all the supported bilayers we have studied so far and may imply that melting of the distal monolayer is a prerequisite to melting of the proximal monolayer. We do not expect the reported results to be particularly sensitive to the specific composition chosen here. The solid-to-liquid transition in the proximal monolayer also starts at the grain boundaries. However, even though the lateral structure is the same, the melting process of the two layers is slightly different: in the distal monolayer, domain edges of high curvature start to melt at slightly lower temperature than straight edge sections. In contrast, all edge sections of proximal monolayer domains initiate melting at the same temperature. The height difference between the solid and liquid domains of the proximal monolayer is 5.6 Å.

Figure 2 shows the fraction, α, of the melted monolayer measured by AFM plotted against temperature for the distal and the proximal monolayer, respectively. Obviously, the mica support stabilizes the solid phase of the proximal monolayer probably through electrostatic interactions resulting in a dehydration of the lipid headgroups. Neither this AFM data nor the DSC data for SUVs are accurate enough to sustain a detailed thermodynamic analysis in terms of the precise location of the phase boundaries for the binary system [9], cf., Fig. 1. However, it is possible to provide a correspondence between the real-space AFM data for the supported bilayer and the thermodynamic DSC data for the SUVs by considering the entire transitional region in terms of an effective van't Hoff enthalpy, ΔH_{vH}, determined from the van't Hoff equation, $\frac{d\ln K}{d(1/T)} = -\frac{\Delta H_{\mathrm{vH}}}{R}$, where the equilibrium constant, $K = A_l/A_s$, is taken to be the ratio of the areas, A_l and A_s, of the liquid and solid part of the monolayer, respectively. A least-squares analysis of the data in Fig. 2 in the transition region for the two monolayers yields ΔH_{vH} of 372 ± 29 kJ mol^{-1} and 1030 ± 26 kJ mol^{-1} for the distal and the proximal monolayer, respectively. The corresponding van't Hoff enthalpy of melting SUVs of the same composition was determined from our DSC data to be 400 ± 5 kJ/mol, i.e., very similar to that of the distal monolayer determined from the AFM measurements. This means that the effect of mica on the proximal monolayer is to move the temperature range in which the transition takes place to higher temperatures and concomitantly to decrease the width of the transition region of the solid-to-liquid transition. In contrast, the distal monolayer is only little affected by the presence of the mica support, and the transition enthalpy is similar to that measured by DSC on SUVs.

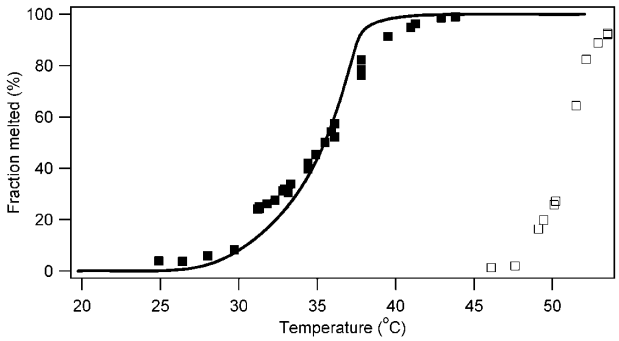

FIG. 2. DSC and AFM data of the solid-to-liquid transition. Filled and empty squares represent AFM data from the distal and the proximal monolayer, respectively. The fraction of melted monolayer (α, measured by AFM) is plotted against temperature. The thick solid line represents the DSC data.

Grain-boundary melting is an interfacial melting process, similar to surface melting and wetting, that takes place at a constrained equilibrium in which the grains do not reorient on the time scale of the melting [10]. Because of the local imperfections of the solid monolayer at the grain boundaries, the melting temperature at the boundaries will be lower than the thermodynamic melting point, T_{m}. The width, $w(T)$, of the interfacially melted region is by mean-field theory [11] predicted to diverge logarithmically, $w(T) \sim -A\ln(T_{\mathrm{m}} - T) + B$, as the temperature approaches T_{m}. By assuming an average hexagonal packing of the grains, we can from the AFM images derive an approximation for the width as $w(T) \sim aN(T)^{-1}A_l/\sqrt{A_s}$, where $a = 3^{1/4}6^{-1/2}$ is a geometric factor and $N(T)$ is the number of grains. Although of limited accuracy and only covering a small temperature range, the resulting data shown in Fig. 3 are found to be in good agreement with the theoretical prediction.

Turning now to the liquid-to-solid transition we find that it is initiated at a number of nucleation sites that appear to

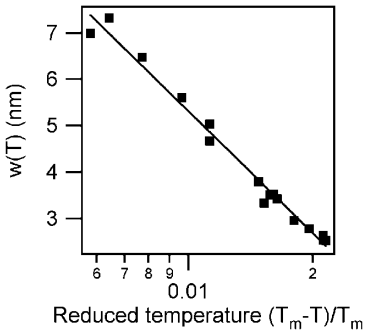

FIG. 3. Semilog plot of the width of the melted interfacial zone $w(T)$ vs reduced temperature $(T_m - T)/T_m$. The straight solid line is the result of a fit of the logarithmic law $w(T) = -A \ln(T_m - T) + B$ to the data. T_m was determined from the fit to be 311.05 ± 0.65 K. This temperature corresponds very well to the temperature where the distal monolayer is completely melted, i.e., the upper limit of the phase coexistence region.

be randomly distributed on the surface [Fig. 1(f)]. These solid nuclei grow until they meet neighboring solid nuclei or where defect lines may form. The resulting solid phase in the proximal monolayer has a lateral structure that resembles the lateral structure in the solid phase proximal monolayer in the heating series [compare Figs. 1(c) and 1(g). When the distal monolayer undergoes the liquid-to-solid transition it is initiated on the defect boundaries of the proximal monolayer but there appear to be fewer nucleation sites than for the proximal monolayer. We observe that when the solid phase of the distal monolayer grows with decreasing temperature, it acquires the same grain-boundary structure as the proximal monolayer.

Our results demonstrate that from the two-component mixture used in our experiments, polycrystalline phospholipid bilayers can easily be prepared and we observe nucleation, domain growth and interfacial melting behavior. The nucleation and growth phenomenon we observe in the liquid-to-solid transition of the proximal monolayer resembles that observed in computer simulations of grain-boundary formation in lipid monolayers [12]. It was actually proposed by these authors that phospholipid bilayers would be ideal candidates for studying interfacial melting provided that polycrystalline bilayers could be prepared. This is in fact what we have found. In the distal monolayer there are fewer nucleation sites and the growth is directed by the underlying grain-boundary structure in the proximal monolayer. We observe that the grain-boundary structure is exactly the same in the two monolayers.

In none of the previous AFM studies on phase transitions in supported bilayers have the results been interpreted as decoupled phase transitions [4–7,13]. However, a closer inspection of the AFM data published in two of those papers [6,7] convinces us that these groups have indeed observed decoupled phase transitions. The presence of salt in the aqueous solution may be a reason why decoupled phase transitions are not always observed. This may be the case for the results reported by Xie *et al.* [4] who conducted their experiments in buffer solution. This further suggests that the interaction between the proximal monolayer and the mica surface is electrostatic in nature. The phosphocholine headgroups are zwitterionic and high salt concentrations may screen the local charges on the surface of both mica and the proximal phospholipid monolayer. The effect of salt has not yet been investigated in the present system. In freestanding bilayers it is observed that the solid domains are symmetric along the normal of the bilayer [14]. Obviously, in supported bilayers this does not always apply and our results may have consequences for the general view on supported bilayers as biologically relevant model systems. We believe that the results reported in this Letter may be of importance when evaluating the use of supported lipid bilayers for nanodevices (e.g., sensors) and for templates to reconstitute functioning membrane proteins and channels [15].

MEMPHYS—Center for Biomembrane Physics is supported by The Danish National Research Foundation. D. K.'s stipend was funded by MEMPHYS and Risø National Laboratory, Roskilde, Denmark. A Grant from the Danish Natural Research Council (to IMM) is gratefully acknowledged.

[1] E. Sackmann, Science **271**, 43 (1996).
[2] L. K. Tamm and H. M. McConnell, Biophys. J. **47**, 105 (1985).
[3] J. Yang and J. Appleyard, J. Phys. Chem. B **104**, 8097 (2000).
[4] A. F. Xie, R. Yamada, A. A. Gewirth, and S. Granick, Phys. Rev. Lett. **89**, 246103 (2002).
[5] F. Tokumasu, A. J. Jin, and J. A. Dvorak, J. Electron Microsc. **51**, 1 (2002).
[6] Z. V. Leonenko, E. Finot, H. Ma, T. E. S. Dahms, and D. T. Cramb, Biophys. J. **86**, 3783 (2004).
[7] M.-C. Giocondi, L. Pacheco, E. Milhiet, and C. L. Grimellec, Ultramicroscopy **86**, 151 (2001).
[8] L. J. Lis, M. McAlister, N. L. Fuller, R. P. Rand, and V. A. Parsegian, Biophys. J. **37**, 657 (1982).
[9] I. P. Sugár, J. Phys. Chem. **91**, 95 (1987).
[10] G. Besold and O. G. Mouritsen, Comput. Mater. Sci. **18**, 225 (2000).
[11] R. Kikuchi and J. W. Cahn, Phys. Rev. B **21**, 1893 (1980).
[12] M. J. Zuckermann and O. G. Mouritsen, Eur. Biophys. J. **15**, 77 (1987).
[13] F. Tokumasu, A. J. Jin, G. W. Feigenson, and J. A. Dvorak, Ultramicroscopy **97**, 217 (2003).
[14] L. A. Bagatolli and E. Gratton, Biophys. J. **79**, 434 (2000).
[15] O. G. Mouritsen, *Life—As a Matter of Fat. The Emerging Science of Lipidomics* (Springer Verlag, New York, 2005).